CSCanada
Advances in Petroleum Exploration and Development
Vol. 20, No. 1, 2020, pp. 54-62
DOI:10.3968/12103

ISSN 1925-542X [Print]
ISSN 1925-5438 [Online]
www.cscanada.net
www.cscanada.org

Analysis of Drill Pipe Failure Mechanism in SHYB-583 Well in Saudi Arabia

CHEN Hongxia[a],*

[a] Sinopec Shengli Petroleum Engineering Co., Ltd., Drilling Technology Research Institute, Dongying. Shandong, China.
*Corresponding author.

Received 3 September 2020; accepted 12 October 2020
Published online 26 December 2020

Abstract
Aiming at the problem of drill pipe washout in the SHYB583 well in Saudi Arabia, the failure mechanism of drill rod is studied by analyzing the physical and chemical properties of thickened transition zone, stress analysis of transition zone under the combined action of tension, bending and torsion, flow field characteristics of inner channel, dynamic characteristics and fatigue analysis of drill string under the condition of actual well trajectory. The results show that the thickness of some parts of the coating of the failed drill pipe sample does not meet the requirements of SY/T 0544-2010 technical conditions for internal coating of petroleum drill pipe (seriously thin), and the drill pipe material contains high index nitride, which reduces the impact toughness of the drill pipe, thus reducing the fatigue life of the drill pipe. Under the combined load, the transition section of the drill pipe has a high stress level, and there is a significant eddy current near the transition zone, and the total pressure of the drill pipe caused by the internal flow field is large. The drill string does not produce more severe whirl, and the amplitude of axial vibration and transverse vibration is small, but the vibration frequency of bending stress is twice of the rotation frequency of the drill string. The large dogleg of the failed drill string increases the bending stress, which makes the drill string more prone to fatigue failure.

Key words: Drill pipe; Physical and chemical characteristics; Stress analysis; Flow field analysis; Dynamic characteristics; Fatigue failure

Chen, H. X. (2020). Analysis of Drill Pipe Failure Mechanism in SHYB-583 Well in Saudi Arabia. *Advances in Petroleum Exploration and Development, 20*(1), 54-62. Available from: http://www.cscanada.net/index.php/aped/article/view/12103
DOI: http://dx.doi.org/10.3968/12103

1. INTRODUCTION
Petroleum drill string is a pipe material with large consumption and high quality requirements in the petroleum industry. It works in a long and narrow borehole filled with drilling fluid, and the force of the drill string in the downhole is very complicated. A large number of drill string failure accidents occur every year at home and abroad, causing significant economic losses[1-2]. The SHYB area in Saudi Arabia has rapid stratum changes, frequent soft and hard interlacing, and strong water sensitivity, which can easily cause instability and reduction of boreholes and other downhole complexities. It is a desert hilly landform. Several small salt lake swamp basins are formed between the sand dunes. Drilling can only be carried out in these small basins. In recent years, multilateral wells and other technologies have been widely used to develop oil and gas resources, and the drilling technology has become more and more perfect. At the same time, due to the complex three-dimensional characteristics of the wellbore trajectory space, the force characteristics of the drill string, especially the dynamic characteristics, are very complicated, and the dynamic safety of the drill string becomes

poor. As shown in Figure 1. During the drilling process of Well SHYB-583, which was drilled in 2012, 8 consecutive washout occurred in the deflection section, which seriously affected the drilling operation. More importantly, the three wells with the same wellhead, SHYB-581, SHYB-582, and SHYB-583 wells all had the same problem, and other wells had similar phenomena. There are many reasons for drill pipe washout[3-6], such as fatigue failure of drill pipe[7], unreasonable design of drill pipe transition zone[8-9], erosion of drilling fluid[10] and many other aspects. This paper aims to find out the failure reason of the drill string based on the analysis of the physical and chemical properties of the thickened transition zone, the stress analysis of the transition zone under the combined action of tension, bending and torsion, and the dynamic characteristics and fatigue analysis of the drill string under the actual wellbore trajectory， and optimize parameters to form technical measures, so as to provide technical reference for safe drilling in oilfield.

(a) (b) (c)

Figure 1
Piercing Drill Pipe in Well SHYB-583

2. RESEARCH ON THICKENING TRANSITION ZONE OF FAILED DRILL PIPE

2.1 Analysis of Physical and Chemical Properties

The specification of puncture failure drill rod was Φ127mm×9.19mm, S135 steel grade. The piercing positions of the drill pipe samples were all the positions where the thickened transition zone disappears, as shown in Figure 1(c). Took two of the drill pipe samples numbered ZYST0398 and ZYST0258 and cut them. The structural features are shown in Figure 2(a) and Figure 2(b). Measured the size of the thickened section of samples ZYST0398 and ZYST0258, the corresponding inner thickened transition zone length (Miu) was 100.5mm and 91.5mm, respectively, and the inner thickened parallel section length (Liu) of the two samples was the same, both were 96.5 mm. All were normal.

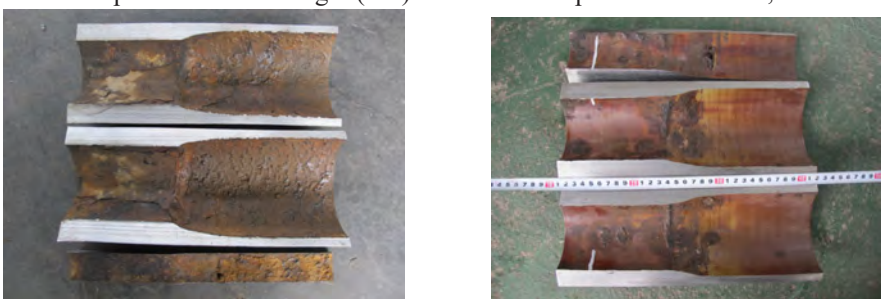

(a) ZYST0398 **(b)** ZYST0258

Figure 2
Structural Characteristics of Thickened End of Drill Pipe Sample with Puncture Failure

2.1.1 Chemical Composition Analysis

Samples were taken around the puncture of samples ZYST0398 and ZYST0258, and a direct-reading spectrometer was used for chemical composition analysis in accordance with ASTM A370. The results are shown in Table 1, indicating that the chemical compositions of the failed samples meet the requirements of API 5DP standard.

Table 1
Chemical Composition Analysis Results (Mass Fraction)

Elements Samples	C	Si	Mn	P	S	Cr	Mo	Ni	V	Al	Cu
ZYST0398	0.23	0.22	1.02	0.016	0.0045	0.47	0.196	0.12	0.008	0.023	0.15
ZYST0258	0.23	0.18	1.02	0.015	0.0052	0.47	0.15	0.09	0.011	0.028	0.18
API 5DP Standard Requirements	-	-	-	≤0.020	≤0.015	--	-	-	-	-	-

2.1.2 Tensile and Impact Properties

According to the ASTM A370 standard, a plate-shaped tensile specimen and a 7.5mm×10mm×55mm impact specimen were taken near the puncture holes of the samples ZYST0398 and ZYST0258, and the test was carried out at room temperature. The results are shown in Table 2. The results show that the yield strength, tensile strength, elongation and impact energy of the failed samples meet the requirements of the API 5DP standard.

Table 2
Tensile and Impact Performance Results of Failed Samples

Properties / Samples	Tensile properties			Impact performance	
	Tensile strength Rm/MPa	Yield strength Rt0.7/MPa	Elongation /A%	Single value	Average
ZYST0398	1064.5	1001.6	20	80,80,76	79
ZYST0258	1017.9	966.4	20.8	76,74,76	75
API 5DP Standard Requirements	≥1000	931~1138	≥13	≥38	≥43

2.1.3 Rockwell Hardness

Took a ring-shaped sample near the puncture hole and conducted a Rockwell hardness test in accordance with ASTM A370. The results are shown in Table 3. The results show that the Rockwell hardness of the samples meet the requirements of the API 5DP standard.

Table 3
Rockwell hardness Test Results

Samples / Measuring Points	1	2	3	4	5	6	7	8	9	10	11	12
SZAR258	33.8	34.0	35.4	32.6	33.7	34.6	31.8	35.7	34.9	33.1	36.7	34.6
S0398	33.3	33.6	33.3	32.2	34.9	35.8	31.7	32.2	33.8	33.5	35.2	34.3
API 5DP Standard Requirements	≤37HRC											

2.1.4 Metallographic Analysis

The metallographic samples were taken in the transverse direction near the puncture holes of samples ZYST0398 and ZYST0258, and the microstructure was observed. The results are shown in Figure 3. The metallographic structure of the samples are all tempered sorbite. Metallographic samples were taken along the longitudinal direction for non-metallic inclusion rating. The results are shown in Table 4. The inclusion content in the structure is within the normal range, but the nitride content is too high.

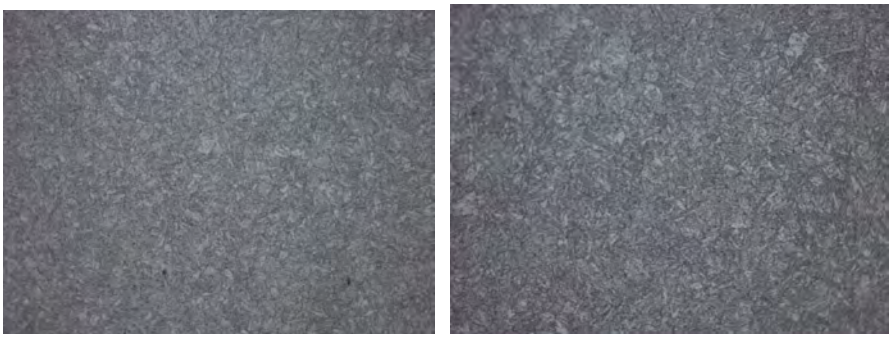

(a) Sample ZYST0258 **(b) Sample ZYST0398**

Figure 3
Metallographic Structure

Table 4
Rating Results of Non-Metallic Inclusions in Steel

Items	A		B		C		D		Ds
	Coarse	Fine	Coarse	Fine	Coarse	Fine	Coarse	Fine	
ZYST0398	0	0.5	0	1.0	0	0	0	0.5	/
ZYST0258	0	1.0	1.5	1.0	0	0	0	1.0	/

2.1.5 Evaluation of Inner Coating of Drill Pipe

Took a longitudinal metallographic sample from the uneven coating of the sample ZYST0258 pipe body and measured the coating thickness. The results are shown in Table 5. The thickness of some parts of the sample coating does not meet the technical requirements of Standard SY/T 0544-2010 for internal coating of petroleum drill pipe.

Table 5
Measurement Results of the Coating Thickness of the Inner Wall of the Drill Pipe

Position	1	2	3	4	5	6	7	8	9
ZYST0258	148	144	137	179	111	100	192	133	118
Requirements of Standard SY/T0544-2010	200±50（150-250）								

2.2 Stress Analysis of Transition Zone

We used the finite element analysis software ABAQUS to establish the three-dimensional mechanical model of the failed drill pipe ZYST0398 and ZYST0258 thickened transition zone, as shown in Figure 4. Fine meshes were used in the transition section, and relatively sparse meshes were used for the rest of the pipe body, thereby constructing a finite element model with high calculation accuracy and high calculation efficiency. A distributing type of nodal coupling was established at the thickened end to apply external loads; a kinematic type of nodal coupling was established at the end of the pipe body to impose constraints. The number of units in the entire model was 475,000 and the number of nodes is 507,000.

Taking into account the influence of dynamic load and the variability of actual working conditions, the load close to the limit working state of the drill pipe was used for calculation and analysis, that is, composite loads such as 3000kN axial tension, 12kNm bending moment and 40kNm torque were used for comprehensive analysis.

Figure 4
Finite Element Model of the Thickened Transition Section

Figure 5 shows the von Mises stress distribution cloud diagram of the thickened transition section of the failed drill pipe ZYST0398 and ZYST0258. It can be seen from the figure that due to the action of bending moment, the stress distribution in the transition zone was uneven, the stress on the compression side of the drill pipe was reduced, and the stress on the tension side was increased. In addition, the rotation torque of the drill string during operation led to the increase of the shear stress in the transition zone section, which further increased the von Mises stress in the thickened transition zone of the drill pipe, and the maximum von Mises stress in the transition zone of ZYST0398 and ZYST0258 drill pipes was 1096MPa.

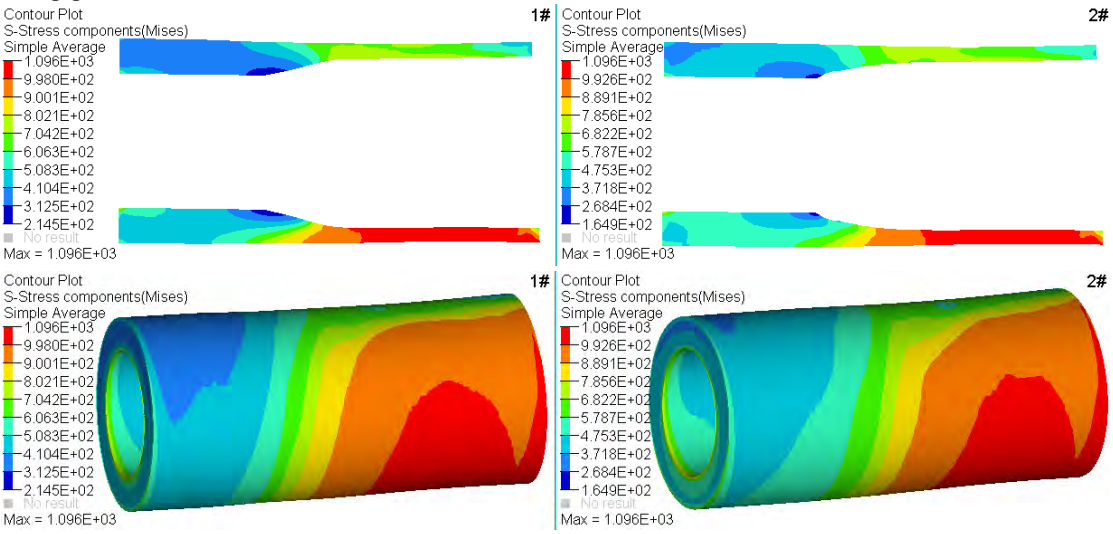

(a) Pipe ZYST0258 **(b) PipeZYST0398**

Figure 5
Von Mises Stress Distribution Cloud Diagram in the Transition Section of Drill Pipe under the Action of Axial Tension, Bending Moment and Rotating Torque

2.3 Flow Field Characteristics of the Flow Channel in the Transition Zone of Failed Drill Pipes

Then used ANSYS to analyze the flow field characteristics of the flow channel in the transition zone between ZYST0398 drill pipe and ZYST0258 drill pipe. The narrow mouth of the pipe was the inlet and the thick mouth was the outlet. The inlet flow rate was 40L/s, the outlet pressure was 0, the liquid density was 1100kg/m^3, and the viscosity was 0.01kg/(m s). According to the model, the minimum diameter, maximum diameter, minimum area, maximum area, the maximum average velocity and minimum average velocity of the pipeline can be calculated, as shown in Table 6.

Table 6
Structural Parameters and Related Parameters

	Min diameter (mm)	Max diameter (mm)	Min area (mm2)	Max area (mm2)	Max average velocity (m/s)	Min average velocity (m/s)
ZYST0258	42.41	54.31	84820	108620	0.472	0.368
ZYST0398	42.81	54.31	85620	108620	0.467	0.368

Figure 6 shows the total pressure diagram of the flow field in the drill pipe corresponding to the samples ZYST0258 and ZYST0398. It can be seen from the figure that when the inlet flow was constant, the total pressure in the flow field inside the two pipes had similar changes. The pressure near the inlet was the highest, the pressure near the transition area was reduced, the pressure on the wide wall of the pipeline was lower, and the pressure near the center of the entire pipeline was greater. Obvious negative pressure appeared near the transition area between ZYST0258 drill pipe and ZYST0398 drill pipe.

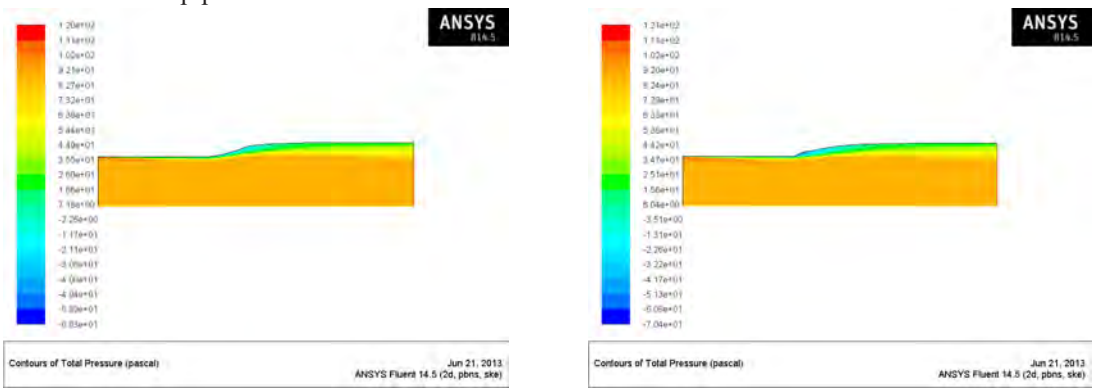

(a) ZYST0258 **(b) ZYST0398**

Figure 6
The total pressure of the sample drill pipe transition zone

Figure 7 shows the curve of the total pressure on the wall of the two types of drill pipes as a function of the respective wall. It can be seen that the wall pressure at the entrance was the largest. From the thin end of the drill pipe to the position where the pipe changes from thin to thick (the beginning of the transition zone), the pressure continued to drop and reaches a negative extreme at the beginning of the transition zone. Then the total wall pressure slowly rose. At the thick end of the pipe, the total wall pressure was about zero.

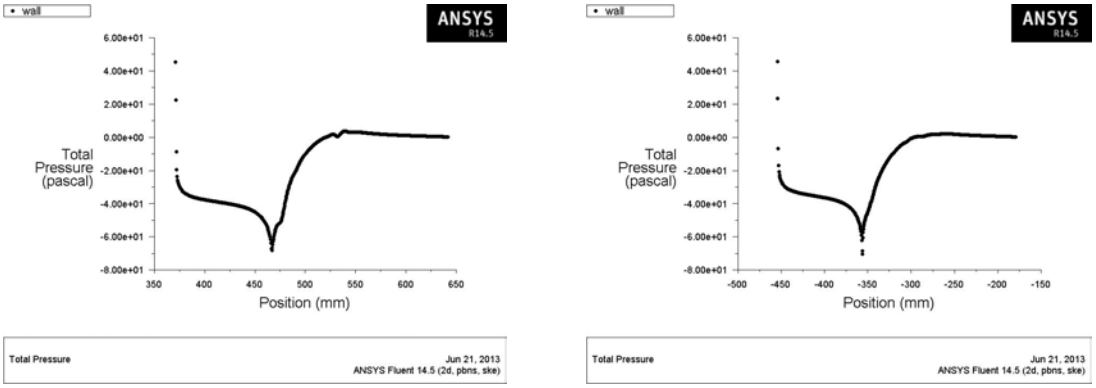

(a) ZYST0258 **(b) ZYST0398**

Figure 7
Pressure Change Diagram of Sample Drill Pipe Transition Zone

Figure 8 shows the X-direction velocity diagram of the flow field in the two drill pipes. It can be seen from the figure

that there were significant vortices (velocities are negative) near the transition zone inside the ZYST0258 drill pipe and ZYST0398 drill pipe; in addition, the maximum X-direction velocity of the two drill pipes appeared near the inner wall of the thin end of the pipe.

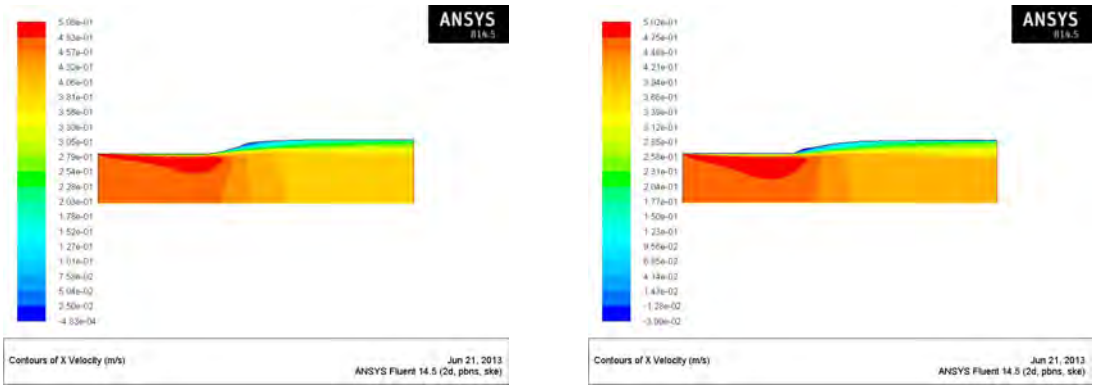

(a) ZYST0258 **(b) ZYST0398**

Figure 8
X-Direction Velocity Diagram of Sample Drill Pipe Transition Zone

3. FULL WELL DRILL STRING DYNAMIC CHARACTERISTICS AND FATIGUE ANALYSIS

The following assumptions are adopted for the drill string dynamics model: (1) The borehole section is round; (2) The drill string is a three-dimensional elastic beam; (3) The influence of the drill string joints is ignored; (4) The deformation of the drill string is regarded as small deformation .

Using Hamilton's principle[3], the nonlinear dynamic finite element equation of the drill string can be established. The dynamic equilibrium equation is generally expressed as[4]:

$$[M]\{\ddot{U}\}+[C]\{\dot{U}\}+[K]\{U\}=\{F\} \quad (1)$$

Among them, $\{\ddot{U}\}$, $\{\dot{U}\}$, $\{U\}$, $\{F\}$ are the generalized acceleration, generalized velocity, generalized displacement and external force vector respectively. $[M]$, $[C]$, $[K]$ are the mass matrix, damping matrix and stiffness matrix respectively.

For the above-mentioned drill string dynamics model, the finite element method was used to solve equation (1). Discrete in space and time[4]. For the discretization of space, the node iteration method was used, and for the discretization of time, the Newmark method was used.

3.1 Analysis of the Dynamic Characteristics of the Drill String

Based on the above model, the dynamic characteristics of the drill string of SHYB-583 when drilling to 3789m was simulated and analyzed. The drilling tool assembly structure was: 215.9mm PDC drill bit + 177.8mm drill collar × 9m + 206.4mm stabilizer + 177.8mm drill collar × 18m + 127mm heavy weight drill pipe × 207m + 127mm drill pipe × 3555m, total 3789m; drilling fluid density is 1160kg/m^3; operating parameters: drilling pressure 70kN, rotating speed 60r/min.

Figure 9 shows the vortex trajectory, vortex velocity and vortex acceleration of the drill string near the puncture leak (the well depth is 927m). It can be seen that the drill string was reciprocating against the lower well wall with a small amplitude because it was in the buildup section, and the overall level of vortex velocity and vortex acceleration was low, and the frequency of vortex acceleration changed faster after 12s.

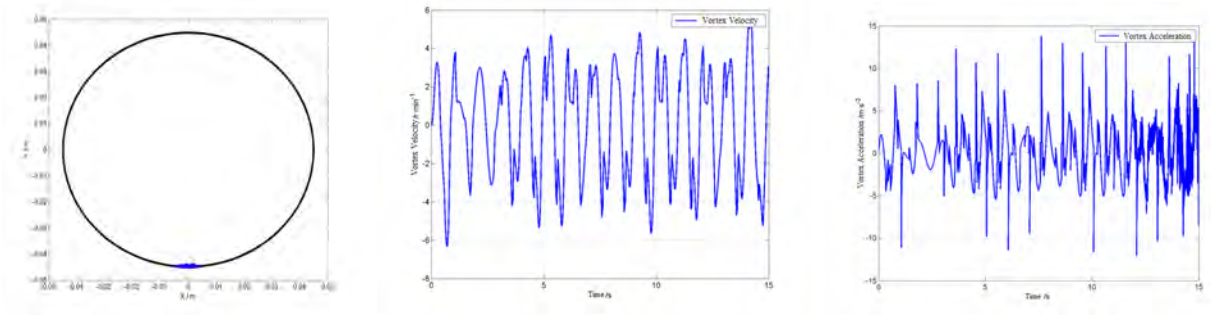

(a) Vortex Trajectory (b) Vortex velocity (c) Vortex acceleration

Figure 9
The Vortex Trajectory, Vortex Velocity and Acceleration of the Drill String Cross-Section Centroid near the Puncture Point (927m)

Figure 10 shows the change in bending stress of the drill string at this section position with time. It can be seen from the figure that within 0~15s, the value of the bending stress of the drill string was relatively small. In 0~12s, the vibration frequency of bending stress was relatively stable (2Hz). In 12~15s, although the vibration frequency is still 2Hz as a whole, within a single cycle, the small-range vibration was obviously intensified, and the frequency reached 30Hz.

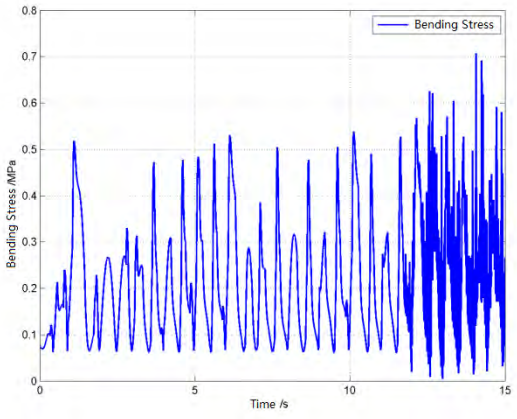

Figure 10
Bending Stress of the Drill String at the Position of the Drill String near the Puncture Point (927m) within 0~15s

3.2 Characteristic Analysis of Static and Dynamic Fatigue Coefficients of Failed Drill Strings

In a wellbore with a certain dogleg degree, the alternation of stress can easily lead to the fatigue failure of drill string. The main source of fatigue failure is the presence of micro-cracks in the crystal structure during material manufacturing. The micro-cracks become larger due to continuous stress (tensile stress or compressive stress) in the drill string. The alternating stress is composed of the constantly changing stress when the drill string rotates, and is mainly divided into bending stress and buckling stress.

This article uses the fatigue analysis model in the literature [6] to analyze the static fatigue characteristics of the drill string in Well SHYB-583. At the same time, the static load in the literature [6] is replaced by the dynamic load, and the dynamic fatigue coefficient R_F^D is obtained.

$$R_F^D = \left(\left|\sigma^D{}_{BUCK}\right| + \left|\sigma^D_{BEND}\right|\right) / \sigma^D_{FL} \qquad (2)$$

In the formula, σ^D_{FL} is the dynamic fatigue limit, which will be embodied as a dynamic variable due to the fluctuation of the dynamic axial force. $\sigma^D{}_{BUCK}$ is the dynamic buckling stress. No drill string buckling occurred in this calculation, so the dynamic buckling stress is not considered. σ^D_{BEND} is the dynamic bending stress, and its calculation formula is:

$$\sigma^D_{BEND} = B\sigma_D \qquad (3)$$

σ_D is the dynamic bending stress calculated by the dynamic model, MPa. B is the bending stress magnification factor (BSMF).

Figure 11 shows the characteristics of the static fatigue coefficient (a) and dynamic fatigue coefficient (b) of the integral drill string of the BA6S well. It can be seen from the figure that the static fatigue coefficient of the drill string is relatively large between the well depth of 500~1000m, and some of it has exceeded 1.0, indicating that for the static drill string, this section of the drill string is prone to fatigue failure under this working condition. On the whole, the dynamic fatigue coefficient of the drill string is basically the same as the static result. The difference is that the fluctuation frequency has increased, reflecting the dynamic characteristics.

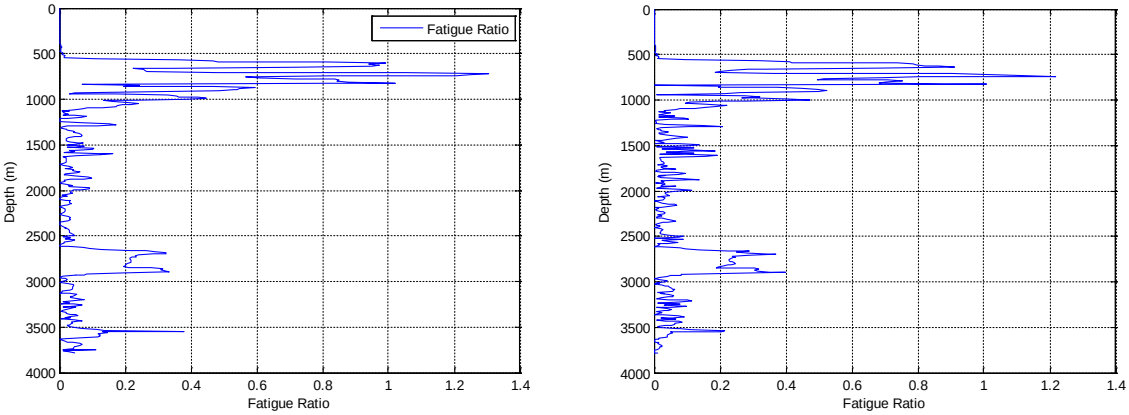

(a) Static Fatigue Coefficient **(b) Dynamic Fatigue Coefficient**

Figure 11
The Characteristics of Static and Dynamic Fatigue Coefficients of the Integral Drill String in Well BA6S

The time-history curve of the dynamic fatigue coefficient of the drill pipe at a well depth of 927m is shown in Figure 12. It can be found that the overall fatigue coefficient has reached 1.2 or more, and the dynamic fatigue coefficient changes frequently between 11~15s, which is mainly caused by bending. It is caused by a higher frequency of stress changes. A higher frequency will make the material reach the fatigue limit faster, leading to failure of the drill string.

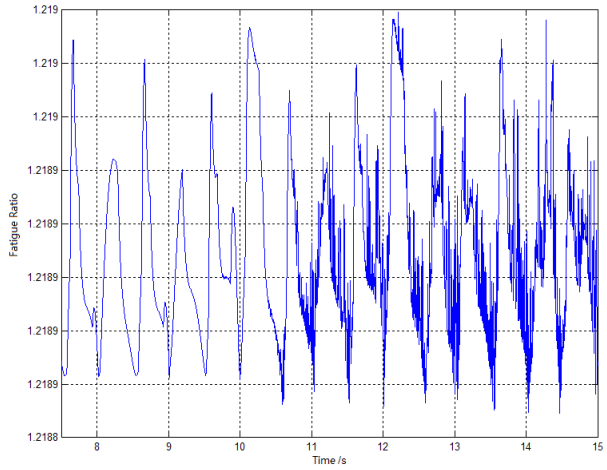

Figure 12
Time-History Curve of the Dynamic Fatigue Coefficient of the Drill String at a Well Depth of 927m

4. CONCLUSIONS

1) The physical and chemical analysis of the drill pipe transition zone shows that the thickness of some parts of the coating of the failed drill pipe sample does not meet the requirements of SY/T 0544-2010 technical requirements for internal coating of petroleum drill pipe (seriously thin), which makes the safety performance of the drill pipe transition

zone have some hidden dangers. The failure drill pipe material contains high nitride (inclusion), which is easy to reduce the impact toughness of drill pipe, thus reducing the fatigue life of drill pipe.

2) The analysis results of stress characteristics of transition zone show that under the combined load, especially under the bending load, the two kinds of failed transition sections of drill pipe have higher stress levels, which increases the risk of failure of the transition section of drill pipe thickening to a certain extent.

3) The analysis of the flow field of the failed drill pipe in the transition zone shows that there is a significant vortex current near the transition zone, and the internal flow field has a large total pressure on the drill pipe, which has a certain impact on the safety of the transition zone.

4) The dynamic calculation results of the well where the drill string failure occurred showed that the drill string did not produce relatively violent turbulence. The drill string in the failed section mainly reciprocated at a small amplitude close to the lower well wall, and the amplitude of axial vibration and lateral vibration was small. However, the vibration frequency of the bending stress is twice the rotation frequency of the drill string..

5) The section of the SHYB-583 well where the drill string fails has a greater dogleg degree, which increases the level of bending stress to a certain extent. After the bending stress amplification factor is further amplified, the drill string in this section is more prone to fatigue invalidate.

6) Based on the above analysis, we replaced the internal coating up-to-standard drilling tools. When drilling similar wells, the quality control of the wellbore has been strengthened to avoid over-design doglegs. We have also strengthened drilling tool replacement and flaw detection work. During the construction of the same block in 2013, the failure of drilling strings decreased significantly.

REFERENCES

[1] – (1992). Failure analysis laboratory of petroleum pipe research center. Investigation report on drilling tool failures in national oilfields in 1988. *OCTG*, (6), 327-336.

[2] Guo, Y. F., Guo, S. S., & Li, H. L. (2003). Preliminary study on the cause of drill pipe leakage in Donghai PH Oilfield. *Foreign Oilfield Engineering,* (04), 32-34.

[3] Lian, Z. H., Luo, F. Q., Gong, J. W., Zhong, S. Q., Liu, Y. Y., & Tang, P. H. (2003). Analysis of drill pipe leakage causes in Tarim Oilfield. *Drilling & Production Technology*, (06), 71-74+8.

[4] Guo, Y. F., Guo, S. S., & Li, H. L. (2004). Research on Pinghu Oil and gas field drill pipe leakage phenomenon. *China Offshore Oil and Gas,* (02), 36-40.

[5] Liu, W. H., Li, L., Liu, Y. G., Pan, Z. Y., & Wang, J. J. (2011). Erosion Failure Mechanism of Pipe Body in Thickened Transition Zone of Drill Pipe Based on Flow Field Analysis. *Journal of Chinese Society for Corrosion and Protection*, (02), 160-164.

[6] Yu, S. J., Yuan, P. B., Gong, D. M., Lu, S. L., & Li, L. Q. (2011). Analysis of the cause of puncture and leakage of S135 drill pipe. *Heat Treatment of Metals,* (S1), 173-177.

[7] Fang, Z. (2006). *Failure analysis of drill pipe*. Southwest Petroleum University.

[8] Liu, W. H., Zeng, Z. X., Li, L., Wang, J. J., Lin, K., & Yang, L. (2010). Study on flow field characteristics of 127mm API drill pipe inner thickening transition zone. *Chinese Journal of Applied Mechanics*, (03), 594-600+651.

[9] Feng, S. B., Lin, Y. H., Shi, T. H., Luo, F. Q., & Zhao, P. (2006). The influence of the geometric structure of the drill pipe thickening transition zone on the stress concentration. *Petroleum Drilling and Production Technology,* (01), 6-78+86.

[10] Zhou, W. D., Xia, B. R., Li, L. P., & Shi, W. (2011). Experimental Study on the Erosion of Drill Pipe Joints by Drilling Fluid. *Petroleum Machinery*, (10), 1-4+195.

[11] Baryshnikov, A., Calderoni, A., Ligrone, A., & Ferrara, P. (2013). A new approach to the analysis of drillstring fatigue behavior. *SPE Drilling & Completion, 12*(02), 77-84.

[12] Dykstra, M. W. (1996). *Nonlinear drill string dynamics*. Tulsa: The University of Tusla.

[13] Hu, Y. B. (2011). *Finite element analysis of drill string dynamic characteristics based on actual borehole trajectory.* Shanghai University.

[14] Paslay, P. R., Corp, T., & Cernocky, E. P. (1991). *Bending stress magnification in constant curvature doglegs with impact on drillstring and casing*. SPE Annual Technical Conference and Exhibition, Society of Petroleum Engineers, pp. 137-146.